

Massive MIMO NOMA with Wavelet Pulse Shaping to Minimize Undesired Channel Interference

Muneeb Ahmad, *Student Member, IEEE*, Soo Young Shin, *Senior Member, IEEE*,

Abstract—In this article, wavelet OFDM based non-orthogonal-multiple-access (NOMA) combined with massive MIMO system for 6G networks is proposed. For mMIMO transmissions, the proposed system could enhance the performance by utilizing wavelets to compensate for channel impairments on the transmitted signal. Performance measures include spectral efficiency, symbol error rate (SER), and peak to average ratio (PAPR). Simulation results prove that the proposed system outperforms the conventional OFDM based NOMA systems.

Index Terms—NOMA, 6G, mMIMO, Imperfect SIC, Wavelet filter banks, FFT-OFDM.

I. INTRODUCTION

FUTURE wireless networks, such as sixth-generation (6G), is projected to enable exceptionally high data rates and a huge number of users with a wide range of applications and services [1]. Massive multiple-input-multiple-output (mMIMO) is considered as one of the most suitable technology for 6G because it provides higher spectral efficiency by allowing its antenna array to focus narrow beams towards a user. Specifically, by deploying a large number of antennas and utilizing the space domain to multiplex various users, the mMIMO technology has the ability to significantly reduce system latency and to deliver exceptional connection improvements. Similarly, the millimeter-wave (mmWave) transmission is considered as another key technology to deliver multi-gigabit-per-second transmission throughput and large data capacity [2]. The availability of a large amount of unlicensed bandwidth that allows for Gigabit data rate transmission is the main attraction to utilize mmWave communication systems. The mmWave frequencies extend from 30 GHz to 300 GHz, where the Federal Communications Commission (FCC) allocated the spectrum of 57–64 GHz, with a carrier frequency of 60 GHz and a bandwidth of 7 GHz for mmWave communication. Various key enabling technologies for mmWave communication are presented in [3].

Non-orthogonal-multiple-access (NOMA) is also proposed as a viable choice for 5G wireless communication networks, in which the transmit power is exploited to segregate the signals of different users [4]. The path loss difference amongst users is utilized to allocate power, where no additional processing is required at the receiver. The user data is multiplexed using superposition algorithm and transmitted through the channel from the base station (BS). At the receiver side, a successive-interference-cancellation (SIC) technique is used to recover the user data. The high power signal is retrieved and subtracted from the received signal that leaves the less power user only to recover and decode its data. While, the high power user

directly recover and decodes its own data by considering less power users' signal as noise [5]. NOMA was proposed as multi-user superposition transmission (MUST) for long term evolution advanced (LTE-A) networks (3GPP version 13), and according to the LTE-A Pro (3GPP release 14), the standardization of NOMA was considered for uplink side, particularly in massive machine type communication (mMTC) [6]. In addition, certain link-level and system-level performance analyses that demonstrate the possibility of implementing NOMA schemes have been carried out in the literature [7].

II. PRIOR WORKS

NOMA and mMIMO were integrated to pave the way for the development of 5G/B5G by enhancing the spectral efficiency (SE), and the energy efficiency (EE) of the cellular networks [8]. The feasibility of NOMA and its performance with the mMIMO setup was first mentioned in [9], where the comparison of conventional mMIMO setup and NOMA was performed in Rayleigh fading channel. Likewise, the NOMA architecture in a multiple-input-single-output (MISO) downlink scenario was studied in [10], where, the effect of quasi-degradation on NOMA downlink transmission was investigated. To increase overall system performance, a low-complexity sequential user pairing method was devised by using the characteristics of hybrid NOMA precoding. Similarly, [11] presented a downlink beamforming (BF) for hybrid NOMA networks to counteract inter and intra-cluster interference.

Fast Fourier transform (FFT) based OFDM multiple access scheme was implemented in the traditional MIMO or mMIMO-NOMA systems, where the exponentially rising data-rate demands have limited the spectrum utilization in the traditional FFT-OFDM based networks. Because, a substantial drawback of FFT-OFDM technique is the limited number of user connectivity to the network due to the limited orthogonal resource allocation and scheduling [12]. Moreover, the sinc function properties of the FFT filter banks form the system makes it more prone to the undesired energy in the side lobes that spills over into the adjacent sub-carriers. In addition, the cyclic prefix (CP) is added to counter the inter user interference and other channel impairments, and this redundancy of CP bits leads to the loss of overall system's throughput and spectral efficiency. On the other hand, a few works present the wavelet OFDM based pulse shaping for NOMA that offers enhanced spectral efficiency, low latency and greater bandwidth [13].

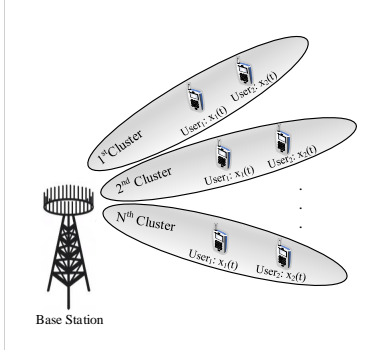


Fig. 1: Cluster Formation and Grouping in mMIMO-NOMA

III. CONTRIBUTION

Because the aforementioned literature study assumed that the number of transmit antennas was either equal to or less than the number of receiving antennas, the appropriate analysis of a mMIMO NOMA system with a large number of transmit antennas was left unaddressed. Moreover, the mMIMO-NOMA setup was not properly analyzed and compared for different pulse shaping techniques to validate the performance comparison of the system. The typical FFT-based pulse shaping for mMIMO setup does not appear to be well suited due to the CP insertion, which causes redundant bandwidth usage. As a result, it may not be the best recourse for 6G wireless communication networks, which demand the highest spectral efficiency and huge data rate.

Similarly, the SIC for NOMA is always assumed to be perfect and the effect of imperfect SIC for mMIMO-NOMA setup is not examined before. To the best of our knowledge, the wavelet based mMIMO-NOMA (mMIMO-WNOMA) system with imperfect SIC with different pulse shaping techniques is not considered before. Therefore, this study presents the mMIMO-WNOMA system to enhance the performance of the 6G wireless communication networks. The performance comparison of the conventional FFT-NOMA with the wavelet pulse-shaped NOMA under mMIMO setup is provided.

Moreover, the concept of wavelet function and its benefits are provided to the multi-user NOMA system to enhance the SER and PAPR. The presented system is also analysed for the real practical scenario under imperfect SIC that leads to the presence of undesired data in the received signal due to the incomplete subtraction of the interference at the intended SIC performing user.

IV. SYSTEM MODEL FOR mMIMO-WNOMA

Consider a downlink mMIMO-NOMA system with multiple antenna at the BS transmitting to the multiple single antenna users. In the presented system, the total number of users (L) are split into clusters (N). The users are kept in an even number for NOMA pairing and are divided into two categories of Near user (x_1) and Far user (x_2). Multiple antenna at the BS are able to direct the beam towards each cluster, as shown in the Fig. 1. The indexes $N_{near} \in N$ ($N_{near} = \{1, 2, \dots, L/2\}$), $N_{far} \in N$ ($N_{far} = \{L/2+1, \dots, L\}$), and ($N = \{1, 2, 3, \dots, L\}$). The classification of users is required for NOMA pairing due

to the channel fading, and it is specifically associated to the large-scale fading effect experienced by the users. In mMIMO-NOMA system, the near and far terms are not absolutely dependent on the distances from the BS in real scenario, rather a far user may have greater large-scale fading due to shadowing compared to the other closer user and may belong to the group index N_{near} . The time-division-duplex (TDD) mode is considered for the presented system because of the channel reciprocity (CR). Utilizing the concept of CR, the BS can estimate the downlink channels subjected to the uplink pilots. Hence, the BS performs the beam-forming based on the channel estimation. Zero-forcing (ZF) beam-forming (BF) is considered in this article, because BF is a general approach to utilize for MIMO network with multiple antenna at the BS. By following the above setup for the system, the BS will transmit the superimposed signal as:

$$x_{n,i} = \sum_{n=1}^N \left(\mathbf{v}_n \sum_{i=1}^2 \sqrt{\alpha_{n,i}} s_{n,i} \right) \quad (1)$$

where, $\alpha_{n,i}$ and $s_{n,i}$ are the allocated power and user data to the i_{th} user in the n_{th} cluster, respectively. \mathbf{v}_n is the pre-coding vector for the desired cluster. NOMA users in the same cluster share the same pre-coding vector but the transmit power is different. The pre-coding vector for the BF is selected to support multiple users in NOMA, as well as to support the SIC process at the near user, because it is susceptible to interference from neighboring clusters. That is why, the BS needs to know the CSI of the near users from all the clusters. However, this type of ZF-BF implementation does not provide array gain to the far user, rather it supports the SIC process and signal recovery at the near and far user, respectively.

V. CONVENTIONAL NOMA AND WAVELET NOMA: A PULSE SHAPING TECHNIQUE

OFDM technique offers various features i.e. lower complexity, less multi-path delay spread, simple channel equalization techniques and interoperability to the existing MIMO networks. For the real environment, the SIC process is not always perfect due to the unknown channel conditions at the BS. That

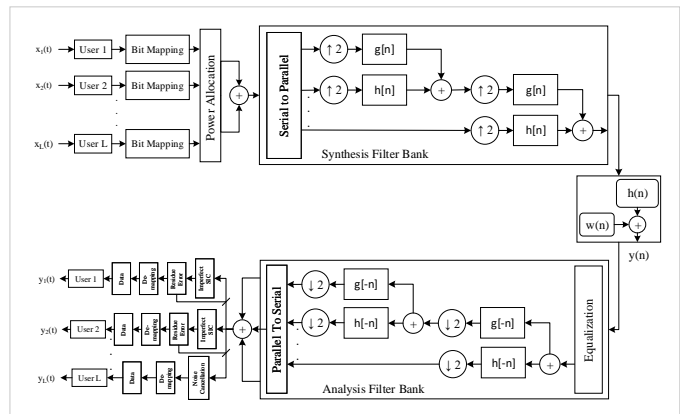


Fig. 2: The Transceiver Structure for multi-user Wavelet based NOMA system: (Residual Error Approach)

is why, the BS is unable to provide the complete channel information about the second group of the users (N_{far}) to the SIC performing group of users (N_{near}) in each cluster. In this situation, the residual error from the initial SIC performing user would spread across the system, degrading the entire signal decoding process.

A general transceiver structure for multi-user wavelet NOMA (WNOMA) is presented in Figure 2, with imperfect SIC effect flowing from the first SIC performing user to the others. After assigning the fractional power to the users's data, the data symbols are subjected to the source coding and modulation. Wavelet pulse shaping is applied at the transmitter side. Multi-carrier modulation in both FFT-OFDM and wavelet-OFDM based NOMA allows multiple low SER data streams over the sub-carriers. Each beam is assigned by a pre-coding vector and directed towards the desired cluster. For NOMA, the near users in each cluster will perform the SIC after passing the signal through both the equalization and analysis filter bank. While, the far users will directly decode the data by treating the near user's interference as noise. The DFT filter banks are applied to the data for FFT-OFDM based NOMA. Because this article analyzes both Fourier and wavelet transformations in the presence of interference due to imperfect SIC and unknown channel conditions, the subsection that follows briefly discusses the reduced effect of interference on wavelet-based NOMA compared to FFT-based NOMA under mMIMO setup.

A. Reduced Interference affect for WNOMA

Compared to the FFT-OFDM, wavelets utilize shorter waveform for orthogonal base and that makes the wavelets robust to reduce the inter-symbol-interference (ISI) and inter-carrier-interference (ICI). ISI occurs when the delayed waves of sub-channel deteriorates the reception of the currently transmitted symbol of the same sub-channel. Whereas ICI occurs due to the orthogonality disturbance of the sub-channels. Thus, both the interferences affect the SIC process due to the mentioned delays in the sub-carrier and the situation even gets worse for the increased sub-carriers. However, the inherent nature of the wavelets of less sensitivity to offsets in both time and frequency domain plays a vital role to reduce these delays. Hence, the delayed symbols from the other sub-channels are successfully clipped out to eliminate the effect of ICI. Moreover, the customize-able characteristics of the wavelets give an extra edge to adapt the channel to reduce ISI. The filter response of both the FFT and wavelets can be seen in Fig. 3(d), where lower power requirements for frequency offsets from interferences and a lower PAPR make wavelet-based system model more resistant to interference from imperfect SIC and aid in improved signal reconstruction under mMIMO setup, therefore boosting the system's SER.

B. Residual error and WNOMA

Traditional NOMA pulse shaping is based on rectangular windows of identical size to the Fourier Transform. While, the wavelet filters in the proposed system utilize inverse discrete wavelet transform (IDWT) and discrete wavelet transform

(DWT) at the transmitter and receiver side, respectively. At the transmitter, the encoded symbols are transformed into the wavelet symbols when passed from synthesis filter banks. The input signal is decomposed into low and high pass components $g[n]$ and $h[n]$, respectively as shown in Fig. 2. Later the IDWT process is performed and the signal can be represented as [12]:

$$x_i = \sqrt{2^{-(J-1)} \frac{E}{T}} \sum_{j \in I} a_j^0 \phi \left(2^{-(J-1)} \frac{t}{T} - j \right) + \sum_{n=1}^{J-1} \sqrt{2^{-(J-n)} \frac{E}{T}} \sum_{j \in I} a_j^n \psi \left(2^{-(J-n)} \frac{t}{T} - j \right) \quad (2)$$

where, E and T are the average symbol energy and the symbol duration respectively. a_j^n is the complex valued M-ary modulated symbol with $n = 0, \dots, j-1$. I is an integer to represent the index set. j is another integer with positive value to show the multi-level decomposition of the wavelets family. Whereas, $\phi(m)$ and $\psi(m)$ is the scaling and wavelet function respectively. Similarly, y_n is the signal propagated over the Rayleigh-Fading channel and received at the n_{th} cluster, and can be shown as:

$$y_n = h_n \sum_{i=1}^2 s_i \sqrt{p_i} + z_n, \quad (3)$$

where, h_n represents the channel for the beam-directed cluster from the BS. s_i and p_i are the i_{th} users' intended signal and power, respectively. z_n is the i_{th} channel link's zero-mean complex additive Gaussian noise with σ^2 as variance. At the receiver end, LS and minimum-mean-square-equalization (MMSE) equalization is considered for the received signal to nullify the channel effect. Later, the signal is passed through the analysis filter bank for wavelet reconstruction with the inverse process applied at the synthesis filter banks. Now the data is subjected to the SIC process.

It is important to mention here that most of the literature study assumed perfect SIC that is one of the key aspect to realize the NOMA gain. While, in a massive MIMO setup, perfect SIC for NOMA is difficult to achieve, since complete channel information at the receiver is not possible in real practice. As a result, for SIC performing users, an imperfect SIC causes unwanted interference in the signal. This unwanted interference is referred to as residual error, and it affects the intended user's SER [14]. Similarly, the flow of residual error through the entire massive MIMO setup can degrade the system's SER performance owing to mass connection as presented in the receiver side of Fig. 2. Therefore, Wavelet filters are preferred here in the presented mMIMO-NOMA system to reduce the influence of residual error since wavelets provide higher resilience to signal distortion caused by unwanted energy as detailed in sub-section III-A. To accomplish this, the received signal is processed in the analysis filter bank, where it is passed through low and high pass filters with impulse response g_n and h_n , respectively. The use of FFT and

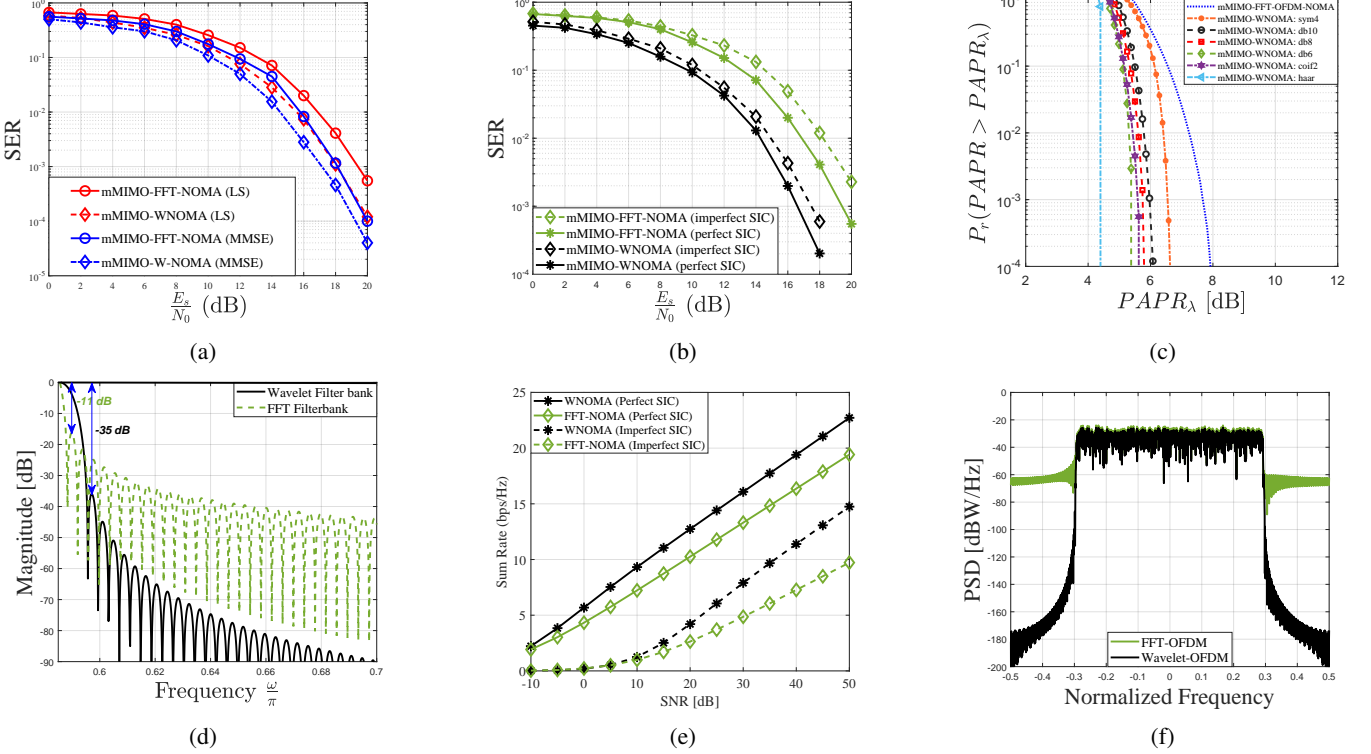


Fig. 3: SER comparison of FFT-OFDM and wavelet-OFDM based massive MIMO-NOMA. (a) LS and MMSE Channel Equalization. (b) Perfect and Imperfect SIC. (c) PAPR comparison of FFT-OFDM with diverse wavelet family. (d) Magnitude Spectra of FFT and Wavelet filter-banks. (e) Capacity comparison of FFT-NOMA and WNOMA. (f) PSD comparison of FFT-NOMA and WNOMA

DWT is a signal's linear transformation procedure. Where, the received signal can be transformed using FFT as follows:

$$\begin{aligned} y(t) &= f_{\text{FFT}}[x(t) + \omega(t)] \\ y(t) &= X(t) + \omega_{\text{FFT}}(t) \end{aligned} \quad (4)$$

Similarly, by applying DWT to the received signal, $y(t)$ may be represented as:

$$\begin{aligned} y(t) &= f_{\text{DWT}}[x(t) + \omega(t)] \\ y(t) &= X(t) + \omega_{\text{DWT}}(t) \end{aligned} \quad (5)$$

where, ω_t comprises the interference caused by the residual error, and channel noise z . $\omega_{\text{FFT}}(t)$ and $\omega_{\text{DWT}}(t)$ is noise output from FFT and wavelet filter banks, respectively.

C. PAPR and Spectral Efficiency for WNOMA

Traditional NOMA system possesses the narrow-band signals that are added constructively, hence this increases the instantaneous peak energy of the signal higher than the average signal power. Moreover, the power amplifier in the hardware creates inter-modulation distortions as well [5]. On the contrary, the PAPR of the wavelet filters is much lesser than the FFT-OFDM because of the energy confinement in frequency domain. According to the definition, the PAPR is the ratio of

peak and average power of the signal ($\frac{\rho_{\text{peak}}}{\rho_{\text{avg}}}$). Thus the PAPR of the wavelet based NOMA signal is expressed as [6]:

$$\text{PAPR} = \frac{\max_n \{ |S_W|^2 \}}{E \{ |S_W|^2 \}} \quad (6)$$

where the factor E represents the average value and the factor \max_n shows the maximum value of time index among all instances. The PAPR of any multi-carrier modulation is dependent on the pulse-shape [14]. The selection of suitable pulse-shaping technique can improve the PAPR of the system and can be represented as

$$\text{PAPR} \leq Q_{\text{max}} |\gamma(m)|^2, \quad (7)$$

where, $\gamma(m)$ is the scaling function of the filters and the Q is the total sub-carriers used.

VI. SIMULATION RESULTS AND PERFORMANCE ANALYSIS

The performance of FFT and wavelet OFDM-based pulse shaping techniques with mMIMO-NOMA setup is evaluated and compared for both perfect and imperfect SIC. The simulation is performed using Matlab 2021(a), and the presented mMIMO setup consider 512 transmit antennas (M) at the BS and 1024 user equipment (L) at the receiving end. For wavelet-based pulse shaping, two level decomposition for wavelet filters and for FFT filter banks, 256 sub-channels are considered. Further, each NOMA cluster consists of two

users, as mentioned in Section-II. Therefore, in these clusters, near and far users' are given channel gain of -10 dB and -5 dB, respectively. Furthermore, the \mathcal{M} – QAM modulation scheme is used for both FFT and wavelet setup, whereas CP and bandwidth ratio for FFT is 20% and 80%, respectively. It is assumed that the channel conditions are partially known to the receiver for Rayleigh Fading channel with additive white Gaussian noise with reference to the PAPR and SER.

Fig. 3(a) presents the SER curves of the traditional NOMA and the proposed WNOMA under mMIMO setup, for the Least Square (LS) and the MMSE technique with perfect SIC conditions. It can be seen that WNOMA outperforms FFT based NOMA in both MMSE and LS channel equalization at the receiver end in Fig. 3(a). It is because of the robustness of WNOMA to the interference from neighbouring sub-carriers. Fig. 3(b) shows the SER under incomplete CSI scenario, that leads the entire system to the imperfect SIC. As the channel conditions are not completely known at the receiver, hence the residual error causes the imperfect SIC and leads to the deteriorated data recovery. It can be seen that the analysis filter banks at the receiver preforms better compared to the most adapted FFT-filter banks for NOMA. WNOMA offers a value of 5.956×10^{-4} of SER at 20 dB under imperfect SIC, but the FFT-NOMA delivers its performance of value 2.28×10^{-3} only. This is because of the less PAPR and lower side lobe energy provided by the wavelets as shown in Fig. 3(c) and Fig. 3(d), respectively. Wavelet filter bank provides -24 dB gain over the FFT-filters and also improves spectral efficiency due to the absence of CP which is the redundancy in FFT-NOMA.

Fig. 3 (c) gives an overview of the PAPR showed by the different wavelets, and it gives an extra degree-of-freedom to choose from the large wavelet family to utilize at the receiver. The symlet-4 and the Haar wavelet has 1.2 dB and 3.4 dB gain over the traditional FFT-NOMA. Whereas, the coiflets-2, daubechies-6, 8 and 10 holds the 2.2, 2.3, 2.1 and 2 dB gain, respectively. Furthermore, the out-of-band (OOB) radiated noise because of the poor FFT-filter response degrades the SER and spectral efficiency, where the wavelet filter is capable to reduce OOB due to its tight filter taps. Therefore, the analysis of the spectral efficiency in terms of the sum-rate is also given in the Fig. 3(e) supported by the power-spectral-density (PSD) plot in Fig 3(f). Furthermore, Fig. 3(f) validates that the WNOMA gives high spectral confinement as it holds PSD of -174.19 dB while the FFT-NOMA holds the value of -64.4 dB. Similarly, under imperfect SIC scenario, the WNOMA and the FFT-NOMA provides 14.7 bps/Hz and 9.7 bps/Hz of sum-rate value, respectively. Therefore, the WNOMA offers the added benefit of delivering reliable communication without the need of CP, and allowing the increased multi-user capacity. The presented analysis verifies the enhanced performance of mMIMO-WNOMA for both imperfect and perfect SIC conditions due to its excellent filter response and lesser bandwidth consumption.

VII. CONCLUSION

In this article, authors present the wavelet NOMA based massive MIMO system for the 6G network. The efficient bandwidth utilization can be achieved by implementing NOMA

with the mMIMO setup and the affect of unknown channel conditions at the receiver can be minimized via wavelet filter banks. The presented results show that WNOMA enables the better data recovery compared to the conventional NOMA under perfect and imperfect SIC. Furthermore, the presented model can improve the capacity of a multi-user mMIMO NOMA system, which can enable high data rates and mass connectivity in a future 6G wireless communication system.

In future works the assumptions can be sought to include more users in a cluster or utilizing the relays for multiple groups in a cluster.

REFERENCES

- [1] J. Zhu, M. Zhao, S. Zhang, and W. Zhou, "Exploring the road to 6g: Abc — foundation for intelligent mobile networks," *China Communications*, vol. 17, no. 6, pp. 51–67, 2020.
- [2] K.-C. Huang and Z. Wang, *Millimeter wave communication systems*. Wiley, 2011.
- [3] W. Hong, Z. H. Jiang, C. Yu, D. Hou, H. Wang, C. Guo, Y. Hu, L. Kuai, Y. Yu, Z. Jiang, Z. Chen, J. Chen, Z. Yu, J. Zhai, N. Zhang, L. Tian, F. Wu, G. Yang, Z.-C. Hao, and J. Y. Zhou, "The role of millimeter-wave technologies in 5g/6g wireless communications," *IEEE Journal of Microwaves*, vol. 1, no. 1, pp. 101–122, 2021.
- [4] O. Maraqa, A. S. Rajasekaran, S. Al-Ahmadi, H. Yanikomeroglu, and S. M. Sait, "A survey of rate-optimal power domain noma with enabling technologies of future wireless networks," *IEEE Communications Surveys Tutorials*, vol. 22, no. 4, pp. 2192–2235, 2020.
- [5] S. Baig, M. Ahmad, H. M. Asif, M. N. Shehzad, and M. H. Jaffery, "Dual phy layer for non-orthogonal multiple access transceiver in 5g networks," *IEEE Access*, vol. 6, pp. 3130–3139, 2018.
- [6] H. Lee, S. Kim, and J.-H. Lim, "Multiuser superposition transmission (must) for lte-a systems," in *2016 IEEE International Conference on Communications (ICC)*, 2016, pp. 1–6.
- [7] A. Khan, M. A. Usman, M. R. Usman, M. Ahmad, and S.-Y. Shin, "Link and system-level noma simulator: The reproducibility of research," *Electronics*, vol. 10, no. 19, p. 2388, 2021.
- [8] S. Kusaladharma, W.-P. Zhu, W. Ajib, and G. A. A. Baduge, "Achievable rate characterization of noma-aided cell-free massive mimo with imperfect successive interference cancellation," *IEEE Transactions on Communications*, vol. 69, no. 5, pp. 3054–3066, 2021.
- [9] K. Senel, H. V. Cheng, E. Björnson, and E. G. Larsson, "Noma versus massive mimo in rayleigh fading," in *2019 IEEE 20th International Workshop on Signal Processing Advances in Wireless Communications (SPAWC)*, 2019, pp. 1–5.
- [10] Z. Chen, Z. Ding, X. Dai, and G. K. Karagiannidis, "On the application of quasi-degradation to miso-noma downlink," *IEEE Transactions on Signal Processing*, vol. 64, no. 23, pp. 6174–6189, 2016.
- [11] Z. Chen, Z. Ding, and X. Dai, "Beamforming for combating inter-cluster and intra-cluster interference in hybrid noma systems," *IEEE Access*, vol. 4, pp. 4452–4463, 2016.
- [12] A. Khan and S. Y. Shin, "Wavelet ofdm-based non-orthogonal multiple access downlink transceiver for future radio access," *IETE Technical Review*, vol. 35, no. 1, pp. 17–27, 2018.
- [13] S. Baig, U. Ali, H. M. Asif, A. A. Khan, and S. Mumtaz, "Closed-form expression for fourier and wavelet transform-based pulse-shaped data in downlink noma," *IEEE Communications Letters*, vol. 23, no. 4, pp. 592–595, 2019.
- [14] M. Ahmad, S. Baig, H. M. Asif, and K. Raahemifar, "Mitigation of imperfect successive interference cancellation and wavelet-based nonorthogonal multiple access in the 5g multiuser downlink network," *Wireless Communications and Mobile Computing*, vol. 2021, p. 1–11, 2021.